

Autocorrelations in the totally asymmetric simple exclusion process and Nagel-Schreckenberg model

Jan de Gier*

Department of Mathematics and Statistics, The University of Melbourne, VIC 3010, Australia

Timothy M. Garoni†

*ARC Centre of Excellence for Mathematics and Statistics of Complex Systems,
Department of Mathematics and Statistics, The University of Melbourne, VIC 3010, Australia*

Zongzheng Zhou

Department of Modern Physics, University of Science and Technology of China, Hefei 230027, PR China

(Dated: January 13, 2010)

We study via Monte Carlo simulation the dynamics of the Nagel-Schreckenberg model on a finite system of length L with open boundary conditions and parallel updates. We find numerically that in both the high and low density regimes the autocorrelation function of the system density behaves like $1 - |t|/\tau$ with a finite support $[-\tau, \tau]$. This is in contrast to the usual exponential decay typical of equilibrium systems. Furthermore, our results suggest that in fact $\tau = L/c$, and in the special case of maximum velocity 1 (corresponding to the totally asymmetric simple exclusion process) we can identify the exact dependence of c on the input, output and hopping rates. We also emphasize that the parameter τ corresponds to the integrated autocorrelation time, which plays a fundamental role in quantifying the statistical errors in Monte Carlo simulations of these models.

PACS numbers: 05.40-a, 05.60cd, 05.70Ln

1. INTRODUCTION

The totally asymmetric simple exclusion process (TASEP) [1] is a simple transport model, of fundamental importance in nonequilibrium statistical mechanics. In addition to its mathematical richness, it has applications ranging from molecular biology to freeway traffic.

A TASEP consists of a chain of length L , with each site being either occupied by a particle or not, on which particles hop from left to right. See FIG. 1. If site $i = 1$ is vacant a particle will enter the system with probability α . If site $i = L$ is occupied the particle will leave the system with probability β . In the bulk of the system, a particle on site i will hop to site $i + 1$ with probability $1 - p$ provided $i + 1$ is vacant, otherwise it remains at site i .

TASEPs exhibit boundary-induced phase transitions, governed by the parameters α , β and p . In general, for a given p , there exist three possible phases, depending on α and β : a low-density phase, a high-density phase, and a maximum-current (or maximum-flow) phase.

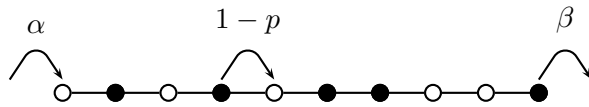
In the context of traffic models it is most appropriate

to update all sites in parallel, at each time-step. The stationary distribution of the TASEP with fully-parallel updates [2, 3] is known exactly. The Nagel-Schreckenberg (NaSch) model [4] is an important generalization of the parallel-update TASEP, in which particles can move up to $v_{\max} \in \mathbb{N}$ sites per time step. The NaSch model is generally considered to be the minimal model for traffic on freeways. While many results are known rigorously for the TASEP, our understanding of the NaSch model and its further generalizations typically rely on numerical simulation. This is particularly true of traffic network models, in which the NaSch model is often a component (see for example [5–7]).

In the current article we focus on dynamic correlation functions. It was recently observed [8] that the TASEP with random sequential update exhibits non-trivial oscillations in the power spectrum of the system density, in the low and high density phases. We further elucidate the nature of these non-trivial oscillations, and demonstrate that they extend to the NaSch model generally.

In addition to the intrinsic physical interest of such phenomena, we emphasize their important practical consequences for the correct design of Monte Carlo simulations. For example, it is common in works describing numerical simulations of the TASEP or NaSch model to read statements such as “we measured observable X every m time steps”. Unless accompanied by an estimate of the integrated autocorrelation time of X , however, such statements contain essentially no information. Indeed, as we discuss in section 2, in order to circumvent the effects of the autocorrelations inherent in Markov-chain Monte Carlo simulations, m must be at least as large as the integrated autocorrelation time. One important practical

FIG. 1: A TASEP with $L = 10$.



*Electronic address: jdgier@unimelb.edu.au

†Electronic address: t.garoni@ms.unimelb.edu.au

consequence of our results is that even when computing the system density of the low or high density (and therefore “non-critical”) NaSch model, the integrated autocorrelation time scales with the system size L . Sampling with a fixed value of m , independent of L , therefore implies a systematic underestimation of statistical errors for large system sizes. Despite the widespread use of the NaSch model in traffic simulations, and the fundamental importance of the system density in such studies, it appears that this result has not been previously reported. Bringing such issues to wider attention is one key motivation of the present article.

Autocorrelation functions for the TASEP with random sequential update have been studied in [8, 9] and display a separation of time scales between relaxation of local density fluctuations and collective domain wall motion. (For reviews of the *stationary* properties of TASEPs with random sequential updates see [10, 11].) For example, an important quantity in many applications, including traffic modeling, is the system density, n , which is simply the fraction of sites which are occupied. The relationship between density and flow is known as the *fundamental diagram* in the traffic engineering literature. While the stationary-state expectation $\langle n \rangle$ of n is known rigorously for TASEP, the dynamic behavior of n_t is non-trivial. Indeed, the power spectrum of n_t for the TASEP with random sequential updates was recently [8] shown to exhibit non-trivial oscillations in the low and high density phases.

In this work we investigate this question numerically in the time, rather than the frequency domain, and for fully-parallel updates. We find a very simple form for the finite-size scaling of the autocorrelation function $\rho_n(t) := (\langle n_0 n_t \rangle - \langle n \rangle^2) / \text{var}(n)$. Up to very small corrections, our numerical simulations for the deterministic limit $p = 0$ strongly suggest that in both the high and low density phases we have

$$\rho_n(t) = \begin{cases} 1 - |t|/\tau, & |t| \leq \tau \\ 0, & |t| \geq \tau \end{cases} \quad (1)$$

for some constant $\tau \propto L$. As discussed in more detail in section 2.5, the Fourier series of $\rho_n(t)$ gives the power spectrum of n , and we note that taking the Fourier series of (1) does indeed produce oscillations as reported in [8]. Indeed, we have simply

$$\sum_{t=-\infty}^{\infty} \rho_n(t) e^{i\omega t} = \frac{1}{\tau} \frac{1 - \cos \tau \omega}{1 - \cos \omega}. \quad (2)$$

While the discussion in [8] focused only on $v_{\max} = 1$, our results suggest that (1) in fact holds for general v_{\max} and is a very good approximation for values of p relevant for traffic modeling.

The specific form (1) of the autocorrelation function has important consequences for the design of Monte Carlo simulations. Indeed, as we show in section 2, assuming the validity of (1), we have $\tau = 2\tau_{\text{int},n}$ where

$\tau_{\text{int},n}$ is the *integrated autocorrelation time* of n . The integrated autocorrelation time can be interpreted loosely as the number of time steps between “effectively independent” samples. It is therefore reasonable to conjecture that the parameter τ should equal the amount of time it takes a perturbation of the stationary state to traverse the system. If we let v denote the speed of such a perturbation then we might reasonably expect that $\tau = L/v$. In section 3 we present numerical results that strongly suggest that in fact, for TASEP, we have

$$\tau = L/|v_c(\alpha, \beta, p)| \quad (3)$$

where $v_c(\alpha, \beta, p)$ is the *collective velocity* [2, 12]. The results (1) and (3) are consistent with the suggestions in [8, 9] that the physical origins of the observed oscillations in the power spectrum of n were related to the time needed for a fluctuation to traverse the entire system.

We note that rescaling $1 - p = \tilde{p}\delta t$, $\alpha = \tilde{\alpha}\delta t$ and $\beta = \tilde{\beta}\delta t$, the fully-parallel update rule becomes equivalent to the random sequential update as $\delta t \rightarrow 0$. Here, $\tilde{\alpha}$ and $\tilde{\beta}$ are the usual injection and extraction rates of the TASEP in continuous time, and one may set $\tilde{p} = 1$ without loss of generality as \tilde{p} just rescales time. While the value of p is therefore irrelevant in the discussion in [8], our results suggest that in fact (3) holds for parallel-update TASEPs with general p .

Furthermore, while no exact expression for $v_c(\alpha, \beta, p, v_{\max})$ seems to be known for the general NaSch model, the scaling form (3) appears to extend to general p and v_{\max} , and for the special case of $p = 0$ our simulations lead us to conjecture a very simple exact relationship between v_c and v_{\max} ; see section 4.

The remainder of this article is organized as follows. In section 2 we briefly review some pertinent general theory relating to autocorrelations, and point out their importance in the context of Markov-chain Monte Carlo simulations, particularly emphasizing the central role played by the integrated autocorrelation time in quantifying the statistical errors inherent in such simulations. We then discuss some theoretical consequences of the specific ansatz (1), and explain its relationship to the results presented in [8]. In section 3 we present our numerical evidence supporting (1) and (3) for TASEP, and also describe the exact expression for $v_c(\alpha, \beta, p)$ in this case. In section 4 we briefly review the definition of the NaSch model before presenting our numerical results for $\rho_n(t)$ in this case. Based on these simulations, we present an expression for v_c in the case $p = 0$, which we conjecture is exact for all v_{\max} . Finally, we conclude in section 5 with a discussion.

2. AUTOCORRELATIONS

Consider a Monte Carlo simulation of an ergodic Markov chain, and assume that sufficient time has passed that the system has reached stationarity. If one now measures an observable X at each time step one obtains a

stationary time series X_1, X_2, \dots . For example, consider a simulation of the NaSch model in which we measure the system density n . The autocovariance function of the time series X_1, X_2, \dots is defined as

$$C_X(t) := \langle X_0 X_t \rangle - \langle X_0 \rangle^2. \quad (4)$$

The expectation $\langle \cdot \rangle$ here is with respect to the stationary distribution, and we note that $C_X(0) = \text{var}(X)$. The corresponding autocorrelation function is then defined in terms of the autocovariance function via

$$\rho_X(t) := \frac{C_X(t)}{C_X(0)}. \quad (5)$$

Typically, one expects that $\rho_X(t)$ decays as an exponential. Finally, assuming $C_X(t)$ to be absolutely summable, its Fourier transform defines the spectral density

$$f_X(\omega) := \sum_{t=-\infty}^{\infty} C_X(t) e^{i\omega t}. \quad (6)$$

2.1. Statistical estimators

We now briefly describe the statistical estimators used to compute the autocorrelation functions from our simulations. Consider a finite stationary time series X_1, X_2, \dots, X_T , and let \bar{X} denote its sample mean. The natural estimator for the autocovariance function $C_X(t)$ is

$$\hat{C}_X(t) := \frac{1}{T-|t|} \sum_{s=1}^{T-|t|} (X_s - \langle X \rangle)(X_{s+|t|} - \langle X \rangle) \quad (7)$$

if the mean $\langle X \rangle$ is known, and

$$\hat{\hat{C}}_X(t) := \frac{1}{T-|t|} \sum_{s=1}^{T-|t|} (X_s - \bar{X})(X_{s+|t|} - \bar{X}) \quad (8)$$

if the mean $\langle X \rangle$ is unknown. We emphasize that, for each t , the estimators $\hat{C}_X(t)$ and $\hat{\hat{C}}_X(t)$ are *random variables*, in contrast to $C_X(t)$, which is simply a *number*. The estimator $\hat{C}_X(t)$ is unbiased, and $\hat{\hat{C}}_X(t)$ is biased by terms of order $1/T$.

The natural estimator for the autocorrelation function $\rho_X(t)$ is

$$\hat{\rho}_X(t) := \frac{\hat{C}_X(t)}{\hat{C}_X(0)} \quad (9)$$

if the mean $\langle X \rangle$ is known, and

$$\hat{\hat{\rho}}_X(t) := \frac{\hat{\hat{C}}_X(t)}{\hat{\hat{C}}_X(0)} \quad (10)$$

if the mean $\langle X \rangle$ is unknown. The estimators $\hat{\rho}_X(t)$ and $\hat{\hat{\rho}}_X(t)$ are both biased by terms of order $1/T$, as a result of the ratios of random variables in (9) and (10).

2.2. Integrated autocorrelation time

From $\rho_X(t)$ we define the integrated autocorrelation time [13] as

$$\tau_{\text{int},X} := \frac{1}{2} \sum_{t=-\infty}^{\infty} \rho_X(t). \quad (11)$$

If \bar{X} denotes the sample mean of X_1, X_2, \dots, X_T then it can be seen that the variance of \bar{X} is proportional to $\tau_{\text{int},X}$ since

$$\text{var}(\bar{X}) = \frac{1}{T^2} \sum_{r,s=1}^T C_X(r-s) \quad (12)$$

$$= \frac{1}{T} \sum_{t=-(T-1)}^{T-1} \left(1 - \frac{|t|}{T}\right) C_X(t) \quad (13)$$

$$\sim 2\tau_{\text{int},X} \frac{\text{var}(X)}{T}, \quad T \rightarrow \infty. \quad (14)$$

It is (14) that accounts for the key role played by the integrated autocorrelation time in the statistical analysis of Markov-chain Monte Carlo time series. If instead of a correlated time series, one considers a sequence of independent random variables, then the variance of the sample mean is simply $\text{var}(X)/T$. It is in this sense that $\tau_{\text{int},X}$ determines how many time steps we need to wait between two “effectively independent” samples. The motivation behind the common statement “measuring observable X every m time-steps” is to avoid the autocorrelations inherent in Markov-chain Monte Carlo simulations, so it follows that we require $m \geq 2\tau_{\text{int}}$.

Returning to the NaSch model, we note that assuming the validity of (1) and (3), it follows immediately from (11) that

$$2\tau_{\text{int},n} = \sum_{t=-\lfloor \tau \rfloor}^{\lfloor \tau \rfloor} \left(1 - \frac{|t|}{\tau}\right), \quad (15)$$

$$= \tau + O(\tau^{-1}) \quad (16)$$

$$= \frac{L}{|v_c|} + O(L^{-1}). \quad (17)$$

If $L/|v_c| \in \mathbb{N}$ then $2\tau_{\text{int},n} = \tau = L/|v_c|$ exactly.

2.3. Exponential autocorrelation time

The exponential autocorrelation time of observable X is defined as

$$\tau_{\text{exp},X} := \limsup_{|t| \rightarrow \infty} \frac{-|t|}{\log \rho_X(t)}, \quad (18)$$

and the exponential autocorrelation time of the system as

$$\tau_{\text{exp}} := \sup_X \tau_{\text{exp},X}, \quad (19)$$

where the supremum is taken over all observables X . The autocorrelation time τ_{exp} measures the decay rate of the slowest mode of the system. All observables that are not orthogonal to this slowest mode satisfy $\tau_{\text{exp},X} = \tau_{\text{exp}}$.

Indeed, consider an irreducible Markov chain on a finite state space with stationary distribution π and initial distribution π_0 . The distribution at time t is then $\pi_0 P^t$. For large t we can bound the distance between $\pi_0 P^t$ and π by [13]

$$d_2(\pi_0 P^t, \pi) \leq e^{-t/\tau_{\text{exp}}} d_2(\pi_0, \pi), \quad (20)$$

where

$$d_2(\nu, \pi) := \sup_{\|f\|_{l^2(\pi)} \leq 1} \left| \int f d\nu - \int f d\pi \right|, \quad (21)$$

and $l^2(\pi)$ denotes the Hilbert space of complex-valued functions defined on the state space of the Markov chain which are square-integrable with respect to π .

The exponential autocorrelation time therefore sets the scale for the number of initial time steps to discard from a simulation, in order to avoid bias from initial non-stationarity.

Returning to the NaSch model, we expect that τ_{exp} is $O(1)$ with respect to L in the high and low density phases. For the TASEP in continuous time (which is comparable to random sequential update), τ_{exp} was computed analytically [14, 15] using the exact Bethe Ansatz solution. For the low and high density regions, the exponential autocorrelation time is a nonzero constant as a function of the system size L , while on the coexistence line $\alpha = \beta$ it scales as L^2 . This scaling is understood from a simple effective domain wall model [12], which performs an unbiased diffusion on the coexistence line. The domain wall picture extends partially into the low and high density phases, and corresponds surprisingly well to the exact result for small values of the boundary rates α and β . This effective model was used in [16] to propose the following expression for τ_{exp} in the low and high density phases

$$\tau_{\text{exp}}^{-1} = D^+ + D^- - 2\sqrt{D^+ D^-} + O(L^{-2}), \quad (22)$$

where

$$D^\pm = \frac{J^\pm}{\rho^+ - \rho^-}, \quad (23)$$

and ρ^\pm and J^\pm are the density and current in the high or low density region of the TASEP with random sequential update. The form (22) was shown to be correct by [14, 15] in some part of the low and high density regions of the phase diagram. A modified domain wall theory is necessary to correctly predict τ_{exp} in all parts of the low and high density regions [15]. Similar arguments should be valid for the TASEP with fully parallel update, but for this case we have not found an exact expression for τ_{exp} of the form (22).

For completeness we add that it is well known that τ_{exp} scales with the KPZ value $L^{3/2}$ in the maximum current phase $\alpha, \beta > 1 - \sqrt{p}$.

Finally, we remark that despite the fact that $\tau_{\text{exp}} = O(1)$ as $L \rightarrow \infty$ in the low and high density phases, the amount of time required for a Monte Carlo simulation to reach approximate stationarity is still expected to have a dependence on L in this case. Indeed, if the initial distribution is unit mass on the empty system, δ , and N denotes the number of occupied sites we have

$$d_2(\delta, \pi) \geq \left| \int N d\pi \right| = \langle n \rangle L. \quad (24)$$

2.4. Finite-size scaling of $\rho_n(t)$

Our simulations, presented in sections 3 and 4 suggest that (1) is a very good approximation for $\rho_n(t)$ in the low and high density phases. However, theoretical considerations suggest that $\rho_n(t)$ cannot actually have a strictly finite support. Indeed, if $\rho_n(t)$ were to have finite support then we would have $-|t|/\log \rho_n(t) = 0$ for all $|t| > \tau$, implying that $\tau_{\text{exp},n} \neq \tau_{\text{exp}}$. This means that $\rho_n(t)$ would not couple to the slowest relaxation mode, which seems unlikely.

To obtain a more precise ansatz for $\rho_n(t)$ we therefore fix some $k \in \mathbb{N}$ satisfying $k \leq \lfloor \tau \rfloor$ and set

$$\rho_n(t) = \begin{cases} 1 - |t|/\tau, & |t| \leq k, \\ B e^{-|t|/\tau_{\text{exp}}}, & |t| \geq k+1. \end{cases} \quad (25)$$

Since we know empirically that (1) is a very good approximation, it must be the case that $k/\tau \sim 1$ as $\tau \rightarrow \infty$. Let us then write $\tau = k + \varepsilon$, where the only assumption we make regarding ε is that $\varepsilon = O(1)$ as $\tau \rightarrow \infty$. Since the continuum limit of $\rho(x\tau)$ should define a continuous function of $x \in \mathbb{R}$ we choose the parameter B by demanding that $1 - |t|/\tau = B e^{-|t|/\tau_{\text{exp}}}$ when $|t| = k$, which yields

$$B = \frac{\varepsilon e^{k/\tau_{\text{exp}}}}{\tau}. \quad (26)$$

With this choice of B we have

$$\rho_n(t) = \begin{cases} 1 - |t|/\tau, & |t| \leq k, \\ \varepsilon e^{-(|t|-k)/\tau_{\text{exp}}}/\tau, & |t| \geq k. \end{cases} \quad (27)$$

Inserting (27) into (11) we now have

$$\begin{aligned} 2\tau_{\text{int},n} &= \sum_{t=-k}^k \left(1 - \frac{|t|}{\tau}\right) + 2 \sum_{t=k+1}^{\infty} \frac{\varepsilon}{\tau} e^{-(t-k)/\tau_{\text{exp}}} \\ &= \tau + \left(\varepsilon(1 - \varepsilon) + \frac{2\varepsilon}{e^{1/\tau_{\text{exp}}} - 1} \right) \frac{1}{\tau}. \end{aligned} \quad (28)$$

Now, $(e^{1/\tau_{\text{exp}}} - 1)^{-1} \sim \tau_{\text{exp}}$ for large τ_{exp} . In section 2.3 however, we argued that in the low and high density

phases $\tau_{\text{exp}} = O(1)$ as $L \rightarrow \infty$ so that the terms arising from the exponential decay of $\rho_n(t)$ are $O(L^{-1})$. Therefore $2\tau_{\text{int},n} = \tau + O(L^{-1})$, just as we obtained from the simple finite-support ansatz (1).

2.5. Power spectra

Given a stationary time series X_1, X_2, \dots, X_T its discrete Fourier transform is defined [17] to be

$$\widehat{X}(\omega) := \frac{1}{\sqrt{T}} \sum_{t=1}^T X_t e^{i\omega t} \quad (29)$$

for $\omega = 2\pi m/T$ with $m = 0, 1, \dots, T-1$. The quantity $|\widehat{X}(\omega)|^2$ is often referred to as the *periodogram* by statisticians [17], and since $\sum_{t=1}^T \exp(-2\pi\pi t i/T) = 0$ for $m \neq 0$ it follows that

$$\begin{aligned} |\widehat{X}(\omega)|^2 &= \sum_{t=-(T-1)}^{T-1} \left(1 - \frac{|t|}{T}\right) \widehat{C}_X(t) e^{-2\pi m t i/T}, \\ &= \sum_{t=-(T-1)}^{T-1} \left(1 - \frac{|t|}{T}\right) \widehat{\widehat{C}}_X(t) e^{-2\pi m t i/T}. \end{aligned} \quad (30)$$

Consequently, it can be shown [17] that for large T we have

$$\left\langle |\widehat{X}(\omega)|^2 \right\rangle = f_X(\omega) + O\left(\frac{1}{T}\right), \quad (31)$$

where the spectral density $f_X(\omega)$ is defined as in (6).

Now we return to the NaSch model. Let N denote the number of occupied sites in the system. The quantity $I(\omega) := T \langle |\widehat{N}(\omega)|^2 \rangle$ is what [8] refer to as the power spectrum of N . They find that for the continuous-time TASEP in the low-density phase

$$\frac{I(\omega)}{T} \approx \frac{2vA}{\omega^2 D} \left[1 - e^{-D\omega^2 L/v^3} \cos\left(\frac{L\omega}{v}\right) \right], \quad (32)$$

where A, D and v are parameters, which [8] set empirically to $v \approx 0.4$, $D \approx 20$ and $A \approx 1/500$.

We now attempt to compare (32) with the corresponding result derived from (1). From (31) we see that $f_N(\omega) \sim \langle |\widehat{N}(\omega)|^2 \rangle$ as $T \rightarrow \infty$, hence we should compare (32) with $f_N(\omega) = L^2 f_n(\omega)$, where $f_n(\omega)$ is computed via (1). Although our empirical observations of the behavior (1) were made in the discrete time case of fully-parallel updates, (1) can be interpreted as a well defined continuous function on \mathbb{R} . To compare with the continuous time result (32) therefore, we compute $f_n(\omega)$ via the continuous-time Fourier transform, so that (1) and (3) predict

$$f_N(\omega) = \frac{2|v_c|}{\omega^2} \text{var}(n) L \left[1 - \cos\left(\frac{L\omega}{|v_c|}\right) \right]. \quad (33)$$

Now, since $\omega = 2\pi m/T$, for sufficiently large T we have $\exp(D\omega^2 L/v^3) \approx 1$. This is exactly the regime used by [8] in their Fig. 3 ($L = 1000$ or $L = 32000$ and $T = 10^6$). Therefore, in this regime we can identify (32) with (33) if $v = |v_c|$ and

$$\frac{A}{D} = \text{var}(n) L. \quad (34)$$

Some remarks are in order. Firstly, for the deterministic limit $p = 0$, the static variance $\text{var}(n)$ can be computed analytically from the known results for the two-point function [3]. In the low density phase it is given by

$$\text{var}(n) = \frac{\alpha(1-\alpha)}{(1+\alpha)^3} \frac{1}{L} + O(L^{-2}), \quad (35)$$

and for the high density region α is replaced by β . We expect that $\text{var}(n) = O(1/L)$ also for $p > 0$ as well as for $v_{\text{max}} > 1$. In general therefore the prefactor in (33) is $O(1)$ in L . Finally, we note that [8] fit (32) to their data with a very small value of A/D . This small value follows from the fact that the numerical simulations in [8] were performed along the mean field line of the TASEP with random sequential update, where, theoretically, $\text{var}(n)$ is identically zero. It is surprising that [8] were still able to extract a meaningful signal on this line.

3. TASEP SIMULATIONS

The stationary distribution of the TASEP with fully parallel updates [2, 3] is known exactly. In particular, if $\alpha < \beta$, $1 - \sqrt{p}$ such TASEPs reside in a low-density phase, while for $\beta < \alpha$, $1 - \sqrt{p}$ a high-density phase results, with $\alpha = \beta < 1 - \sqrt{p}$ defining a coexistence line of the two phases (corresponding to a first order phase transition). For $\alpha, \beta > 1 - \sqrt{p}$ by contrast, the system resides in a maximum-current phase, in which the density is precisely $1/2$.

Before presenting the results of our simulations we discuss the exact form of the collective velocity $v_c(\alpha, \beta, p)$. It was shown in [2] that in all phases of the parallel-update TASEP the current (flow) J and bulk density ρ_b satisfy the relation

$$J = \frac{1}{2} \left(1 - \sqrt{1 - 4(1-p)\rho_b(1-\rho_b)} \right). \quad (36)$$

The *collective velocity* [12] is the drift of the center of mass of a momentary local perturbation of the stationary state, and is related to J and ρ_b via

$$\begin{aligned} v_c &= \frac{\partial J(\rho_b)}{\partial \rho_b} \\ &= \frac{(1-p)(1-2\rho_b)}{\sqrt{1-4(1-p)\rho_b(1-\rho_b)}}. \end{aligned} \quad (37)$$

Let us now define, for convenience, the function

$$f(x, p) = \frac{(1-p)((1-x)^2 - p)}{(1-x)^2 + p(2x-1)}. \quad (38)$$

If we insert into (37) the exact expression [2] for ρ_b in the low-density phase,

$$\rho_b = \frac{\alpha(1-\alpha)}{1-p-\alpha^2}, \quad (39)$$

we find that $v_c(\alpha, \beta, p) = f(\alpha, p)$. A similar argument can be applied to the high-density phase and we find $v_c(\alpha, \beta, p) = -f(\beta, p)$. The negativity of the collective velocity in the high-density phase is due to the fact that it is the propagation of holes from right to left, rather than of particles from left to right, that is important in this phase.

Using these exact expressions for v_c the expression (3) now becomes

$$\tau = \begin{cases} L/f(\alpha, p) & \alpha < \beta, 1 - \sqrt{p}, \\ L/f(\beta, p) & \beta < \alpha, 1 - \sqrt{p}. \end{cases} \quad (40)$$

We note that for $p = 0$ we have $|v_c| = 1$ identically throughout the high and low density regimes so that we simply have $\tau = L$ in this case. We also note that in the low-density (high-density) phase τ is independent of β (α).

We now turn our attention to our Monte Carlo simulations. We simulated the parallel-update TASEP at a variety of values of α, β and p corresponding to both the low and high density phases, for system sizes $L = 10^3, 5 \times 10^3$ and 10^4 . Each simulation consisted of $10^4 L/v_c$ iterations, with the first $10^3 L/v_c$ time-steps discarded to ensure negligible bias due to initial non-stationarity (initially the system was empty). Assuming the validity of (3) this implies we generated $1.8 \times 10^4 \tau_{\text{int}, n}$ samples of the stationary distribution in each simulation. The theoretical discussion in section 2.3 suggests that an initial discard of $10^3 L/v_c$ time steps should in fact provide a highly conservative guard against initialization bias. Empirical plots of the time series of n support this.

The system density n is defined as

$$n := \frac{1}{L} \sum_{i=1}^L n_i, \quad (41)$$

where $n_i \in \{0, 1\}$ denotes the occupation of site i . For each simulation, we measured n at each iteration, and from the resulting time series we estimated the autocorrelation function $\rho_n(t)$ using (10). FIG. 2 shows a finite-size scaling plot of $\rho_n(t)$ assuming the ansatz given by (1) with $\tau = L$, in the $p = 0$ case. The agreement is clearly very good, and the sharpness of the cusp at $t = L$ suggests that any corrections to the ansatz (1) are very small.

FIGs. 3 and 4 show finite-size scaling plots of $\rho_n(t)$ for $p = 0.25, 0.5$, assuming the ansatz given by (1) and (40).

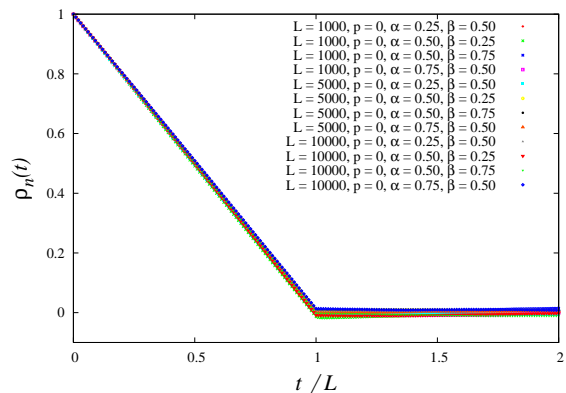


FIG. 2: Color online. Finite-size scaling plot of $\rho_n(t)$ for $p = 0$ parallel-update TASEP in the high-density and low-density phases, for $L = 10^3, 5 \times 10^3, 10^4$ and a variety of α, β .

There is again excellent data collapse, however we note that there is some noticeable curvature near the edge of the support, so that the sharp cusp present in the $p = 0$ case becomes smoothed out somewhat for $p > 0$. As discussed in section 2.4, this does not affect the use of (17) for setting Monte Carlo error bars, but it would be interesting from a theoretical perspective to better understand how this curvature depends on the model parameters p, α, β and L (as well as v_{max} ; c.f. the discussion in section 4). We remark that many other quantities (including the fundamental diagram) have cusps at $p = 0$ which are smoothed out for $p > 0$.

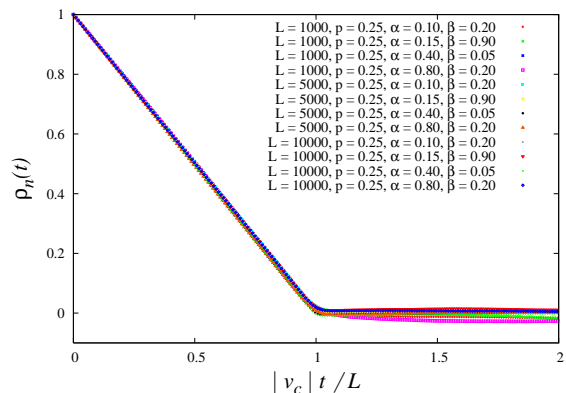


FIG. 3: Color online. Finite-size scaling plot of $\rho_n(t)$ for $p = 0.25$ parallel-update TASEP in the high-density and low-density phases, for $L = 10^3, 5 \times 10^3, 10^4$ and a variety of α, β . The choices of α, β shown correspond to four distinct values of v_c providing strong evidence for the conjecture (40).

4. NAGEL-SCHRECKENBERG MODEL

An important generalization of the TASEP is the Nagel-Schreckenberg model [4], in which each particle

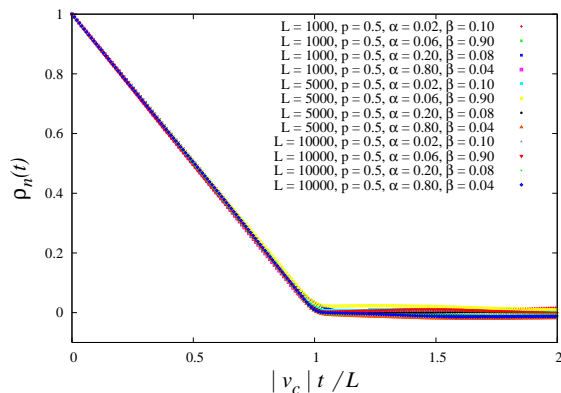


FIG. 4: Color online. Finite-size scaling plot of $\rho_n(t)$ for $p = 0.5$ parallel-update TASEP in the high-density and low-density phases, for $L = 10^3, 5 \times 10^3, 10^4$ and a variety of α, β . The choices of α, β shown correspond to four distinct values of v_c providing strong evidence for the conjecture (40).

(vehicle) can move up to $v_{\max} \in \mathbb{N}$ sites per iteration. Although the precise form of the phase diagram depends on v_{\max} , the NaSch model exhibits, in general, the same three qualitatively distinct phases as TASEP. We now briefly review the dynamical rules defining the NaSch model. Suppose at time $t \in \mathbb{N}$ a vehicle with speed $v_t \in \{0, 1, \dots, v_{\max}\}$ is located on site x_t , and has *headway* (number of empty sites to its right) equal to h_t . Then the maximum speed this vehicle can safely achieve at the next time step is taken to be $v_{\text{safe}} = \min(v_t + 1, v_{\max}, h_t)$, which allows for unit acceleration provided the speed limit is obeyed and crashes are avoided. Provided $v_{\text{safe}} > 0$, a random deceleration is then applied so that with probability p the new speed is $v_{t+1} = v_{\text{safe}} - 1$, otherwise $v_{t+1} = v_{\text{safe}}$. Finally, in the bulk of the system, the vehicle hops v_{t+1} sites to its right, so that $x_{t+1} = x_t + v_{t+1}$. All vehicles in the bulk of the system are updated in this way in parallel. The bulk dynamics clearly reduces to parallel-update TASEP when $v_{\max} = 1$.

It remains to consider the boundary dynamics. We again wish to apply open boundary conditions, however choosing an appropriate implementation of such boundary conditions for the NaSch model is actually surprisingly subtle, and has been an active topic of research over recent years [18–23]. In particular, it was argued in [21] that in order to observe the maximum-current phase when $v_{\max} > 1$ one needs to implement the inflow of vehicles into the system in a rather careful manner.

Since our interest in the present context is confined to the high and low density phases however, we have chosen to implement the boundary conditions in the following simple way. We augment the system, which has sites $1 \leq i \leq L$, with two boundary sites; one at $i = 0$ and another at $i = L + 1$. With probability α a vehicle with speed v_{\max} is inserted on site 0, and we immediately compute v_{safe} for this vehicle. If $v_{\text{safe}} > 0$ we move the vehicle to site v_{safe} otherwise we delete it. The output is performed

similarly. With probability $1 - \beta$ we insert a vehicle on site $L + 1$, which then acts as a blockage to vehicles exiting the system. If the rightmost vehicle in the system has $x_t \geq L - v_{\max}$ we define its new speed to be v_{safe} and attempt to move the vehicle to site $x_{t+1} = x_t + v_{\text{safe}}$. If $x_{t+1} > L$ the vehicle is removed from the system. When $v_{\max} = 1$ the above prescription reduces to the boundary rules for the simple TASEP described in section 1.

We now describe our simulations of the NaSch model as defined above. To our knowledge, no rigorous results are known for v_c when $v_{\max} > 1$, however based on the results of our simulations we conjecture that when $p = 0$ we have

$$v_c = \begin{cases} v_{\max}, & \text{low density phase,} \\ -1, & \text{high density phase,} \end{cases} \quad (42)$$

for any v_{\max} . Indeed, Fig. 5 presents a finite-size scaling plot of $\rho_n(t)$ obtained by simulating the $p = 0$ NaSch model with $v_{\max} = 3$, with system sizes $L = 10^3, 5 \times 10^3$ and 10^4 and a variety of values of α, β corresponding to both the low and high density phases. The data collapse is excellent, providing strong evidence for the ansatz obtained from (1), (3), and (42). As for the case of $p = 0$ when $v_{\max} = 1$ we note the sharpness of the cusp at $t = L/|v_c|$, again suggesting that any corrections to the ansatz (1) are very small. Each simulation performed

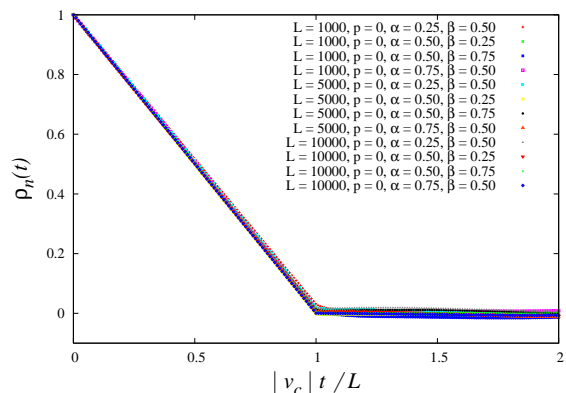


FIG. 5: Color online. Finite-size scaling plot of $\rho_n(t)$ for $p = 0$ NaSch with $v_{\max} = 3$ in the high-density and low-density phases, for a variety of choices of α, β and L . The exact value of v_c is unknown in this case but here we chosen v_c according to (42).

consisted of $10^4 L/|v_c|$ iterations (with v_c given by (42)), with the first $10^3 L/|v_c|$ time-steps discarded.

We remark that the form (42) is intuitively quite reasonable, since in the low-density phase we expect that it is the movement of vehicles from left to right which controls the dynamics, while in the high-density phase we expect that it is the movement of holes (traveling with speed 1) from right to left which is important. The above simulations were also performed for $v_{\max} = 5$ with identical results.

Finally, we also considered the case of $v_{\max} = 3$ with $p = 0.25$. For $v_{\max} > 1$ and $p > 0$ we are not aware of any exact predictions for v_c , however it seems reasonable to conjecture that v_c is independent of β (α) in the low (high) density phase. We therefore simulated the NaSch model with $v_{\max} = 3$, $p = 0.25$ and $\alpha = 0.05$ at four different values of $\beta > \alpha$, which should then correspond to a single value of v_c . By considering a single value of v_c we can still use a finite-size scaling plot of $\rho_n(t)$ to test the conjectures (1) and (3). Fig. 6 provides strong evidence to support their validity at $v_{\max} > 1$ and $p > 0$. By varying the value of $|v_c|$ used to produce the scaling plot of $\rho_n(t)$ so that the support edge lay at $|v_c|t/L = 1$ we obtained $v_c \approx 2.75$. We remark that, assuming the validity of (1) and (3), this method can be used as a way to obtain approximate values of $|v_c|$ when $v_{\max} > 1$ and $p > 0$. Each simulation used in Fig. 6 consisted

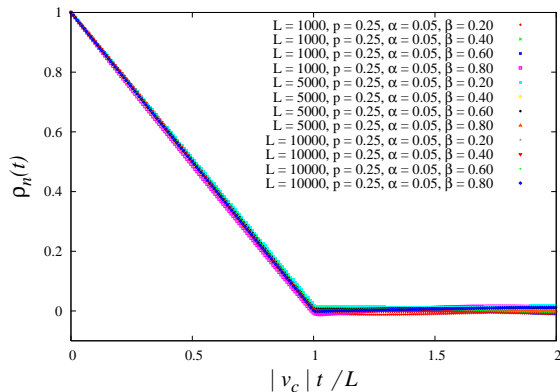


FIG. 6: Color online. Finite-size scaling plot of $\rho_n(t)$ for $p = 0.25$ NaSch with $v_{\max} = 3$ in the high-density and low-density phases, for a variety of choices of α, β and L . The exact value of v_c is unknown in this case but here we have set $v_c = 2.75$.

of $10^4 L/c$ iterations with the first $10^3 L/c$ time-steps discarded, with c set to 3. Since the results of the simulation

suggested that in fact $v_c \approx 2.75 \approx 3$ the statistical errors of these simulations are of a comparable size to the other simulations presented in this article.

We note that unlike the $v_{\max} = 1$ case (see Figs. 3 and 4) there is no noticeable smoothing of the cusp at the support edge in Fig. 6. It therefore appears that the deviations from (1) when $p > 0$ are stronger when $v_{\max} = 1$ than $v_{\max} = 3$, however the physical reason for this is not clear to us.

5. DISCUSSION

We have studied the NaSch model in the low and high density phases via Monte Carlo simulation, and found that to a very good approximation the autocorrelation function for the system density behaves as $1 - |v_c|t/L$ with a finite support $[-L/|v_c|, L/|v_c|]$, where v_c is the collective velocity. For the case of $v_{\max} = 1$ an exact theoretical result is known for v_c for all $p \in [0, 1]$. When $v_{\max} > 1$ no rigorous results for v_c are known, however we conjecture that when $p = 0$ we simply have $v_c = v_{\max}$ in the low-density phase and $v_c = -1$ in the high-density phase. This result agrees with the exact result in the special case of $v_{\max} = 1$ and with numerical simulations for $v_{\max} = 3, 5$. We conjecture that it is valid for all v_{\max} for the $p = 0$ NaSch model with fully-parallel updates.

An important consequence of this form for $\rho_n(t)$ is that $\tau_{\text{int},n}$, and hence the size of Monte Carlo error-bars for n , scale like L . Furthermore, we demonstrated that this result is unchanged if the finite support is replaced by exponential decay at late times.

Acknowledgments

This research was supported by the Australian Research Council. TMG would like to thank Alan Sokal for some useful comments.

-
- [1] F. Spitzer, *Adv. Math.* **5**, 246 (1970).
 - [2] J. de Gier and B. Nienhuis, *Phys. Rev. E* **59**, 4899 (1999).
 - [3] M. R. Evans, N. Rajewsky, and E. R. Speer, *J. Stat. Phys.* **95**, 45 (1999).
 - [4] K. Nagel and M. Schreckenberg, *Journal de Physique* **2**, 2221 (1992).
 - [5] J. Esser and M. Schreckenberg, *Internat. J. Modern Phys. C* **8**, 1025 (1997).
 - [6] M. Schreckenberg, L. Neubert, and J. Wahle, *Future Generation Computer Systems* **17**, 649 (2001).
 - [7] N. Cetin, K. Nagel, B. Raney, and A. Voellmy, *Comput. Phys. Comm.* **147**, 559 (2002).
 - [8] D. A. Adams, R. K. P. Zia, and B. Schmittmann, *Phys. Rev. Lett.* **99**, 020601 (2007).
 - [9] P. Pierobon, A. Parmeggiani, F. von Oppen, E. Frey, *Phys. Rev. E* **72**, 036123 (2005).
 - [10] B. Derrida, *Physics Reports* **301**, 65 (1998).
 - [11] G. M. Schütz, *Phase Transitions and Critical Phenomena*, vol. 19 (Academic Press, London, 2001).
 - [12] A. B. Kolomeisky, G. Schütz, E. B. Kolomeisky, and J. P. Straley, *J. Phys. A: Math. Gen.* **31**, 6911 (1998).
 - [13] A. D. Sokal, in *Functional Integration: Basics and Applications*, edited by C. DeWitt-Morette, P. Cartier, and A. Folacci (Plenum, New York, 1997), pp. 131–192.
 - [14] J. de Gier and F. H. L. Essler, *Phys. Rev. Lett.* **95**, 240601 (2005).
 - [15] J. de Gier and F. H. L. Essler, *J. Stat. Mech.* p. P12011 (2006).
 - [16] M. Dudzinski and G. M. Schütz, *J. Phys. A: Math. Gen.* **33**, 8351 (2000).
 - [17] R. H. Shumway and D. S. Stoffer, *Time Series Analysis and Its Applications* (Springer, New York, 2006), 2nd ed.

- [18] S. Cheybani, J. Kertész, and M. Schreckenberg, Phys. Rev. E **63**, 016107 (2000).
- [19] S. Cheybani, J. Kertész, and M. Schreckenberg, Phys. Rev. E **63**, 016108 (2000).
- [20] Ding-wei Huang, Phys. Rev. E **64**, 036108 (2001).
- [21] R. Barlovic, T. Huisinga, A. Schadschneider, and M. Schreckenberg, Phys. Rev. E **66**, 046113 (2002).
- [22] N. Jia and S. Ma, Phys. Rev. E **79**, 031115 (2009).
- [23] T. Neumann and P. Wagner, Phys. Rev. E **80**, 013101 (2009).